





## Instrumentation

Thermogravimetric analysis (TGA) and elemental analysis were performed at the University of Manchester Microanalytical Laboratory, using a Thermo Scientific Flash 2000 organic elemental analyser and a Seiko SSC/S200 under  $N_2$ . TGA profiles were acquired from room temperature to 600 °C with a heating rate of 10 °C  $min^{-1}$ . Electron microscopy was performed using an FEI XL-30 scanning electron microscope (SEM) in a secondary electron configuration.  $^1H$  NMR spectra were collected using a Bruker AVANCE III 400 MHz spectrometer. X-ray diffraction (XRD) patterns were acquired with a Bruker D8 Advance diffractometer equipped with a Cu  $K\alpha$  source.

## Results and discussion

### Precursor characterisation

The structure of bis[*N,N*-diethyl-*N'*-2-naphthylthioureato]lead(II) is shown in Fig. 1 and Table 1. The structure exhibits a stereo-



Fig. 1 A thermal ellipsoid plot representing the structure of 4. CCDC ref. 1005699.†

Table 1 Selected bond lengths and angles for 4

Bond or angle	Value
Pb(1)–S(1)	2.7080(13) Å
Pb(1)–S(2)	2.6996(12) Å
O(1)–Pb(1)	2.394(3) Å
O(2)–Pb(1)	2.450(3) Å
O(2)–Pb(1)–S(1)	76.09(9)°
S(2)–Pb(1)–S(1)	100.38(4)°



Fig. 2 TGA of 4 & 3 shown as (a) & (b) respectively.

chemically active inert pair resulting in a distorted square pyramidal structure. The structure is similar to that of the previously reported bis[*N,N*-diethyl-*N'*-2-naphthoylselenoureato]



Fig. 3 XRD analysis of the  $PbS_xSe_{1-x}$  films. (a) XRD patterns from  $x_{Se} = 0$  (black),  $x_{Se} = 0.25$  (red) and  $x_{Se} = 0.5$  (blue). (b) XRD patterns of the 422 reflection from  $x_{Se} = 0$  to 0.5. (c) Shows a plot of mole fraction against the position of the 422 reflection as compared to the values from the reference patterns (PbSe ICDD 00-006-0354 and PbS ICDD 00-005-0592) shown with dashed lines.





lead(II) with the exception of the Pb–S bonds being on average 0.8 Å shorter than their Pb–Se equivalents.<sup>8</sup>

The TGA profiles show considerable differences between the breakdown of the sulphur (a) and selenium (b) precursors, Fig. 2. From the first derivatives of the TGA profiles, ESI Fig. 1,† it can be seen that bis[*N,N*-diethyl-*N'*-2-naphthoylthioureato]lead(II), (a), has an onset at 146.3 °C and a three step decomposition whereas bis[*N,N*-diethyl-*N'*-2-naphthoylselenoureato]lead(II), (b), has a higher onset temperature at 210.6 °C and a two-step decomposition. This difference in the number of steps is surprising considering the similarities between the complexes.

### AACVD of mixtures of 3 & 4

The XRD patterns of all the compositions displayed cubic patterns as expected for PbE solids. Fig. 3(a) shows three patterns all showing a cubic pattern with shifts in all reflections across the patterns as the selenium content is increased. Inspection of the 422 reflection over increments of  $x_{\text{Se}} = 0.05$  is shown in Fig. 3(b). The gradual shift in the 422 reflection can be seen from that of pure PbS,  $x_{\text{Se}} = 0$ , to pure PbSe,  $x_{\text{Se}} = 0.5$ . The movement across the entire mole fraction range is shown in

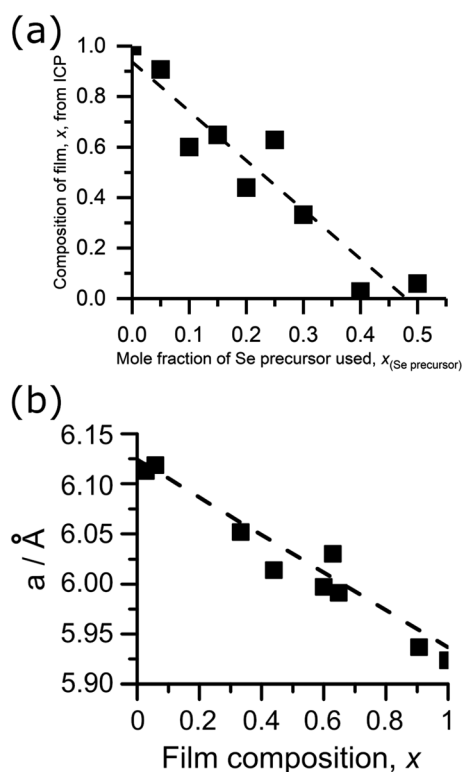


Fig. 4 (a) A plot showing the relationship between the mole fraction of the precursor used and the resulting composition of the film of  $\text{PbS}_x\text{Se}_{1-x}$ . (b) A Vegard plot for the  $\text{PbS}_x\text{Se}_{1-x}$  films between the mole fraction of the Se precursor,  $x_{\text{Se precursor}}$ , 0 to 0.6. Composition of the produced films was determined by ICP-AES analysis of Pb and Se. The dashed line represents ideal Vegardian behaviour between PbS and PbSe using  $a$  from ICDD PbSe 00-006-0354 and ICDD PbS 00-005-0592.

Fig. 3(c). A linear relationship between the mole fraction of the precursors in the CVD flask and the position of the 422 reflection can be observed between  $x_{\text{Se}} = 0$  and 0.4. From  $x_{\text{Se}} = 0.5$  to 1 the 422 reflection matches with the position in the PbSe reference pattern (ICDD 00-006-0354) indicating that the bis[*N,N*-diethyl-*N'*-2-naphthoylthioureato]lead(II) is no longer being incorporated into the films. Linear regression of the region between  $x_{\text{Se}} = 0$  and 0.4 results in a minimum  $x_{\text{Se}}$  of 0.43 for pure PbSe.

Comparison of the film composition by ICP-AES with the lattice constant,  $a$ , allows for examination in relation to Vegard's law, Fig. 4. The films exhibited a linear change in the lattice parameter with decreased sulphur content. This matches with the predicted behaviour of  $\text{PbS}_x\text{Se}_{1-x}$  which is expected to show a subtle deviation from linear behaviour.<sup>27</sup>

Scanning electron micrographs show dramatic variations in the size and shape of the nanocrystals formed when altering the precursor mole fraction as shown in Fig. 5. Variation in the nanocrystal size could be a consequence of the difference in the initial breakdown temperature of the two complexes as shown in the TGA profiles, Fig. 2. The PbSe samples, *i.e.* where

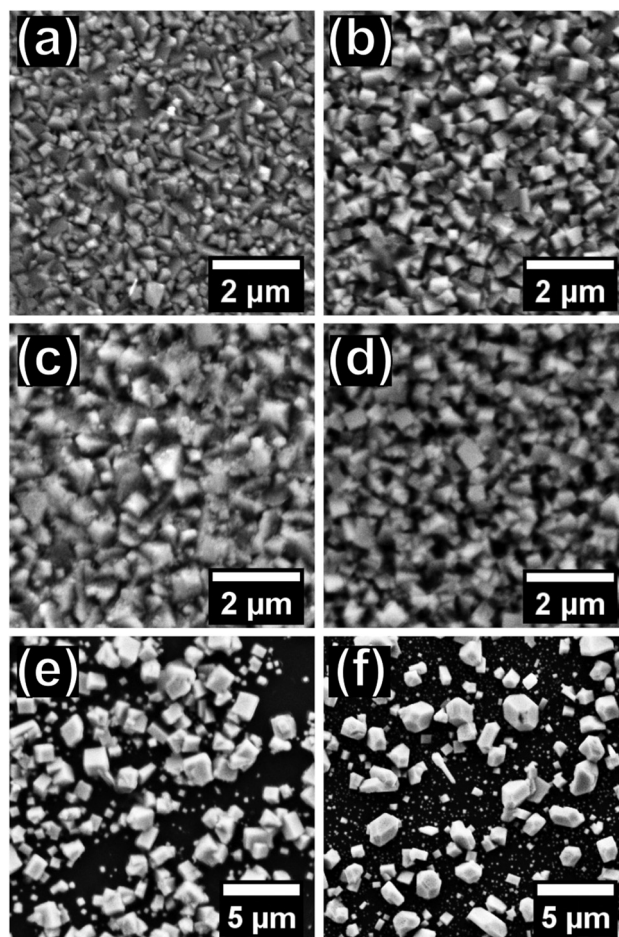
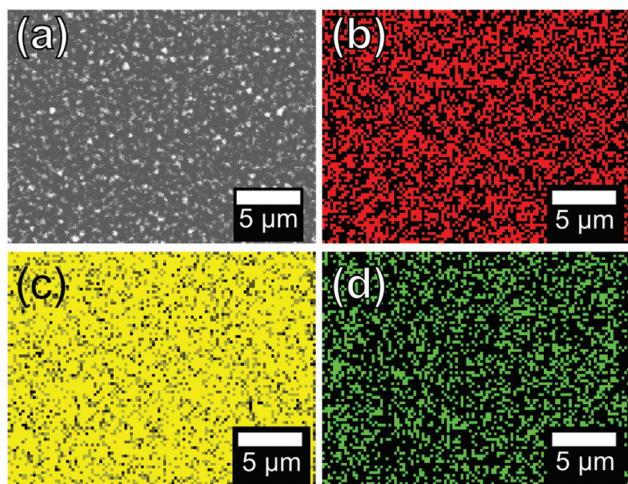


Fig. 5 Scanning electron micrographs of  $\text{PbS}_x\text{Se}_{1-x}$  films produced from  $x_{\text{Se precursor}} = 0, 0.1, 0.2, 0.3, 0.4, 0.5$  and 0.6 represented by (a) to (f) respectively.





**Fig. 6** An SEM image for the alloyed films produced using  $x_{\text{Se (precursor)}} = 0.3$  (a) and the corresponding EDX maps for Pb, S and Se (b), (c) and (d) respectively.

$x_{\text{Se (precursor)}}$  is 0.5 & 0.6 (e & f), show distinctly larger nanocrystals and less uniform films. EDX mapping was used to confirm that a uniform alloy was made, Fig. 6, with Pb, S and Se being found evenly spread across the film. Photographs of the films showed the typical dark brown colour when moving through the range of compositions of the  $\text{PbS}_x\text{Se}_{1-x}$  films, ESI Fig. 2.†

## Conclusions

AACVD of bis[*N,N*-diethyl-*N'*-2-naphthoylthioureato]lead(II) and bis[*N,N*-diethyl-*N'*-2-naphthoylselenoureato]lead(II) mixtures has successfully been used to make  $\text{PbS}_x\text{Se}_{1-x}$  films of controlled chalcogen compositions. The combination of precursors successfully makes alloyed nanocrystals and not two populations of nanocrystals of binary lead chalcogenide compositions. The precursors used performed as ideal single source precursors for AACVD due to the absence of additional undesired phases from the other elements present in the precursor. The relationship between the mole fraction of bis[*N,N*-diethyl-*N'*-2-naphthoylselenoureato]lead(II),  $x_{\text{Se}}$ , and the position of the 422 reflection is linear between  $x_{\text{Se}} = 0$  and 0.43.

## Conflicts of interest

There are no conflicts to declare.

## Acknowledgements

POB and PDM would like to acknowledge funding from the Engineering and Physical Sciences Research Council (EPSRC) grants # EP/K010298/1 and EP/K039547/1. TEE and POB would

like to thank the Nigerian Government for the PhD studentship that supported TEE.

## Notes and references

- N. O. Boadi, M. A. Malik, P. O'Brien and J. A. M. Awudza, *Dalton Trans.*, 2012, **41**, 10497–10506.
- N. L. Pickett and P. O'Brien, *Chem. Rec.*, 2001, **1**, 467–479.
- M. A. Malik, M. Afzaal and P. O'Brien, *Chem. Rev.*, 2010, **110**, 4417–4446.
- M. Afzaal, K. Ahmad and P. O'Brien, *J. Mater. Chem.*, 2012, **22**, 12731–12735.
- M. Afzaal, K. Ellwood, N. L. Pickett, P. O'Brien, J. Raftery and J. Waters, *J. Mater. Chem.*, 2004, **14**, 1310–1315.
- T. Trindade and P. O'Brien, *Chem. Vap. Deposition*, 1997, **3**, 75–77.
- M. J. Moloto, N. Revaprasadu, G. A. Kolawole, P. O'Brien and M. A. Malik, *S. Afr. J. Sci.*, 2005, **101**, 463–465.
- J. Akhtar, M. Akhtar, M. A. Malik, P. O'Brien and J. Raftery, *J. Am. Chem. Soc.*, 2012, **134**, 2485–2487.
- J. Akhtar, M. A. Malik, S. K. Stubbs, P. O'Brien, M. Helliwell and D. J. Binks, *Eur. J. Inorg. Chem.*, 2011, **2011**, 2984–2990.
- M. Akhtar, J. Akhtar, M. A. Malik, F. Tuna, M. Helliwell and P. O'Brien, *J. Mater. Chem.*, 2012, **22**, 14970–14975.
- N. O. Boadi, P. D. McNaughten, M. Helliwell, M. A. Malik, J. A. M. Awudza and P. O'Brien, *Inorg. Chim. Acta*, 2016, **453**, 439–442.
- J. S. Ritch, T. Chivers, K. Ahmad, M. Afzaal and P. O'Brien, *Inorg. Chem.*, 2010, **49**, 1198–1205.
- A. C. Onicha, N. Petchsang, T. H. Kosel and M. Kuno, *ACS Nano*, 2012, **6**, 2833–2843.
- T. Duan, W. Lou, X. Wang and Q. Xue, *Colloids Surf., A*, 2007, **310**, 86–93.
- L. Bolundut, I. Haiduc, G. Kociok-Khön and K. C. Molloy, *Rev. Roum. Chim.*, 2010, **55**, 741–746.
- N. Pradhan, B. Katz and S. Efrima, *J. Phys. Chem. B*, 2003, **107**, 13843–13854.
- J. Akhtar, M. Afzaal, M. A. Vincent, N. A. Burton, I. H. Hillier and P. O'Brien, *Chem. Commun.*, 2011, **47**, 1991–1993.
- J. M. Clark, G. Kociok-Kohn, N. J. Harnett, M. S. Hill, R. Hill, K. C. Molloy, H. Saponia, D. Stanton and A. Sudlow, *Dalton Trans.*, 2011, **40**, 6893–6900.
- P. D. McNaughten, J. C. Bear, A. G. Mayes, I. P. Parkin and P. O'Brien, *R. Soc. Open Sci.*, 2017, **4**, 170383.
- P. D. McNaughten, S. A. Saah, M. Akhtar, K. Abdulwahab, M. A. Malik, J. Raftery, J. A. M. Awudza and P. O'Brien, *Dalton Trans.*, 2016, **45**, 16345–16353.
- E. A. Lewis, P. D. McNaughten, Z. Yin, Y. Chen, J. R. Brent, S. A. Saah, J. Raftery, J. A. M. Awudza, M. A. Malik, P. O'Brien and S. J. Haigh, *Chem. Mater.*, 2015, **27**, 2127–2136.



- 22 J. Akhtar, M. A. Malik, S. K. Stubbs, P. O'Brien, M. Helliwell and D. J. Binks, *Eur. J. Inorg. Chem.*, 2011, **2011**, 2984–2990.
- 23 S. A. Saah, P. D. McNaughten, M. A. Malik, J. A. M. Awudza, N. Revaprasadu and P. O'Brien, *J. Mater. Sci.*, 2018, **53**, 4283–4293.
- 24 I. B. Douglass, *J. Am. Chem. Soc.*, 1937, **59**, 740–742.
- 25 I. B. Douglass and F. B. Dains, *J. Am. Chem. Soc.*, 1934, **56**, 1408–1409.
- 26 G. M. Sheldrick, *Acta Crystallogr., Sect. A: Found. Crystallogr.*, 2008, **64**, 112–122.
- 27 Naeemullah, G. Murtaza, R. Khenata, N. Hassan, S. Naeem, M. N. Khalid and S. Bin Omran, *Comput. Mater. Sci.*, 2014, **83**, 496–503.

